Adsorption of Cr(VI) in wastewater using magnetic multi-wall carbon nanotubes

Zhuo-nan Huang [a,b,*], Xiao-ling Wang [a,b], De-suo Yang [a,b]

[a] *Key Laboratory for Phytochemistry of Shaanxi Province, Baoji University of Arts and Sciences, Shaanxi 721013, PR China*
[b] *College of Chemistry and Chemical Engineering, Baoji University of Arts and Sciences, Shaanxi 721013, PR China*

Abstract

Magnetic multi-wall carbon nanotubes were prepared with wet chemical treatments and characterized by a transmission electron microscope (TEM) and X-ray diffraction (XRD). They were used as adsorbents for the removal of Cr(VI) in aqueous solutions. The effects of adsorbent dosage, the concentration of Cr(VI) in aqueous solution, temperature, and pH value on the removal efficiency were studied. Results showed that the adsorption capacity of the magnetic multi-wall carbon nanotubes increased with the initial Cr(VI) concentration, but decreased with the increase of adsorbent dosage. The adsorption amount increased with contact time. The adsorption kinetics were best represented by the pseudo second-order kinetic model, and the adsorption isotherms indicated that the Langmuir model better reflected the adsorption process. The obtained calculation results for the Gibbs free energy revealed that the adsorption was a spontaneous and endothermic process. The enthalpy deviation was $3.835 \text{ kJ} \cdot \text{mol}^{-1}$. The magnetic multi-wall carbon nanotubes showed significant potential for application in adsorption of heavy metal ions.
© 2015 Hohai University. Production and hosting by Elsevier B.V. This is an open access article under the CC BY-NC-ND license (http://creativecommons.org/licenses/by-nc-nd/4.0/).

Keywords: Magnetic multi-wall carbon nanotubes; Cr(VI); Adsorption; Kinetics; Thermodynamics

1. Introduction

Because most inorganic and organic contaminants do not undergo degradation, they cause major threats to the environment and human health (Gupta et al., 2006). Inorganic contaminants often have certain degrees of toxicity depending on the particular oxidation state. One such contaminant is chromium, which is widely used in industrial activities such as electronic components manufacturing, paint manufacturing, mechanical alloying, tanning of animal hides, metallurgical alloying, and pulp processing (Benhammou et al., 2007). Different processes that are involved in these industrial activities expose many workers to dangerous and high amounts of chromium, which can cause chromium poisoning (O'Brien et al., 2003). Chromium primarily exists in two oxidation states in the environment, Cr(VI) and Cr(III). Cr(VI) forms that dominate in the water are $HCrO_4^-$, CrO_4^{2-}, and $Cr_2O_7^{2-}$. Cr(VI), which is highly soluble and mobile in the aquatic environment, is toxic to both plants and animals, and is regarded as a suspected carcinogenic agent. The toxicity of Cr(VI) is approximately 100 times that of Cr(III) (Yao et al., 2008).

A number of technologies for the removal of inorganic and organic contaminants from aqueous solutions have been developed over years, including ion exchange (Shaidan et al., 2012), adsorption (Mittal et al., 2010b), chemical precipitation (Altas and Büyükgüngör, 2008), photocatalytic degradation (Gupta et al., 2007a), membrane filtration (Juang and Shiau, 2000), and electrochemical methods (Gupta et al., 2007b).

Of these, adsorption is considered the one with the most potential due to its high efficiency and strong ability for removing contaminants (Mittal et al., 2005). Adsorption is a simple treatment process requiring less investment and creating no biological sludge secondary pollution (Ahalya et al., 2003). New practices have been focused on searching for efficient adsorbents.

As a new carbon material, carbon nanotube (CNT) has a large specific surface area and high reaction activity, which aid in the adsorption of heavy metals and organic contaminants in solutions (Mauter and Elimelech, 2008; Lu and Chiu, 2006; Li et al., 2003; Rahbari and Goharrizi, 2009; Di et al., 2004; Tawabini et al., 2010; Ren et al., 2011). However, for ordinary CNT, there exist problems including a small particle size, poor dispersion ability, and difficulty in separation. Moreover, there is resistance to flow when CNT is used as a solid-phase extraction sorbent to treat water samples, which restricts its application in wastewater treatment. Gupta et al. (2011a) have investigated the adsorption behavior of alumina supported on CNT for the treatment of lead aqueous solutions and found that the coated CNT exhibited better removal ability than the uncoated CNT.

In recent years, magnetic separation technology has gradually become the focus of scientists' concern. It has been applied in many fields, including medicine, analytical chemistry, cell biology, and environmental technology (Ngomsik et al., 2005). The prepared magnetic CNT can be well dispersed in water and easily removed from the medium with the help of a magnet (Madrakian et al., 2011). Removal of inorganic and organic contaminants using magnetic CNT as an adsorbent has been reported. Tarigh and Shemirani (2013) have synthesized magnetic multi-wall CNT (MWCNT) nanocomposite as an adsorbent for the removal of Pb(II) and Mn(II). Gong et al. (2009) prepared magnetic MWCNTs for removal of cationic dyes from aqueous solution. Qu et al. (2008) developed MWCNTs filled with Fe_2O_3 particles for removal of methylene blue and neutral red dyes. Tang et al. (2012) produced magnetic MWCNT as an adsorbent for the removal of atrazine and Cu(II) from an aqueous solution simultaneously. Currently, there are many studies employing magnetic CNTs to remove pollutants from wastewater, but little information concerning the interaction between Cr(VI) and magnetic MWCNTs has been reported.

The main objective of the study was to examine the adsorption behavior of magnetic MWCNTs with respect to Cr(VI). Factors, such as contact time, adsorbent dosage, temperature, and pH value were investigated. The kinetics and thermodynamics of Cr(VI) adsorption by the magnetic MWCNTs were also studied.

2. Experimental setup

2.1. Materials

MWCNTs were purchased from Shenzhen Nanotech Port Co., Ltd. The average diameters of the MWCNTs were 20−40 nm, the length was 2 μm, and the specific surface area was 200 $m^2 \cdot g^{-1}$. All other agents were of analytical grade, and purchased from Tianjin Kemiou Chemical Reagent Co., Ltd. The water used in the test was double distilled water. All glassware was soaked in dilute hydrochloric acid for 12 h and finally rinsed three times in double distilled water prior to use.

2.2. Wet chemical treatments of magnetic MWCNTs

The magnetic MWCNTs were prepared according to the method in Gupta et al. (2011b) with some modifications. Typically, MWCNTs were purified through refluxing in concentrated nitric acid at 60°C for 12 h, with the impurities removed through stirring, and then washed with double distilled water until the pH value reached 6.0. The samples were dried at 100°C for 8 h. Subsequently, 1.0 g purified MWCNTs were suspended in 200 mL of mixed solution containing 1.7 g $(NH_4)_2Fe(SO_4)_2 \cdot 6H_2O$ and 2.51 g $NH_4Fe(SO_4)_2 \cdot 12H_2O$. A certain amount of NH_4OH was added into the suspension at 50°C with a nitrogen atmosphere and sonicated for 10 min. The pH value of the final suspension was controlled in the range of 11−12 during a 30-min reaction. After the reaction, the product magnetic MWCNTs were separated from the mixture with a permanent magnet, washed three times with deionized water and alcohol, respectively, and then dried overnight at 60°C in a vacuum oven.

2.3. Adsorption procedure

Adsorption experiments of Cr(VI) by magnetic MWCNTs were carried out in the batch mode. An amount of 0.1 g adsorbent was added to a 150 mL conical flask filled with 100 mL of chromate solution with a concentration of 2 $mg \cdot L^{-1}$. The solution was agitated at 500 rpm over different time periods. The aqueous phase was separated with a 0.45 μm acetate membrane filter. The amount of Cr(VI) in the filtrate solution was measured with a spectrophotometer.

The adsorption efficiency E is calculated using Eq. (1):

$$E = \frac{C_0 - C_e}{C_0} \times 100\% \tag{1}$$

where C_0 and C_e are the initial and equilibrium concentrations of Cr(VI) ($mg \cdot L^{-1}$), respectively.

The adsorbed amount of Cr(VI) under equilibrium conditions, q_e, is calculated using Eq. (2):

$$q_e = \frac{(C_0 - C_e)V}{W} \tag{2}$$

where V is the solution volume (L), and W is the adsorbent dosage (g).

3. Results and discussion

3.1. Transmission electron microscope (TEM) morphology of magnetic MWCNT

TEM images of the MWCNT and magnetic MWCNT, as shown in Fig. 1, revealed that iron oxide nanoparticles are
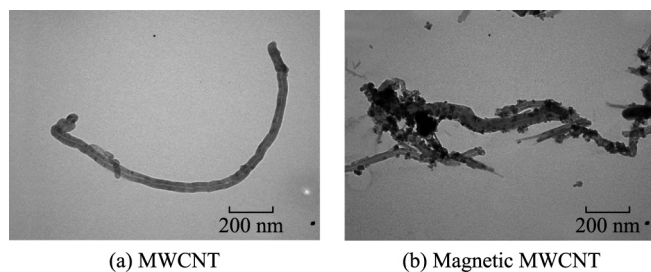
(a) MWCNT   (b) Magnetic MWCNT

Fig. 1. TEM images of MWCNT and magnetic MWCNT.

Fig. 3. Effect of adsorbent dosage on Cr(VI) adsorption by magnetic MWCNTs.

successfully coated on the surface of MWCNTs or encapsulated into the interiors of MWCNTs to form magnetic nanocomposites. Because the capillary tube force of MWCNTs can overcome the surface tension of water, Fe^{2+} and Fe^{3+} entered the MWCNTs and Fe_3O_4 was prepared in situ. In addition, MWCNTs were cut off by nitric acid oxidation and formed open ends, which also helped iron ions to enter the interiors of MWCNTs and to be adsorbed on the surface of MWCNTs.

Fig. 2 illustrates the X-ray diffraction (XRD) patterns of the MWCNT and magnetic MWCNT, where 2θ is the diffraction angle. The observed indices of crystal planes (hkl values), 220, 311, 422, 511, and 440 confirm the cubic structure of Fe_3O_4. It is evident from the figure that Fe_3O_4 and MWCNTs co-exist in the magnetic MWCNTs.

3.2. Effect of adsorbent dosage on Cr(VI) adsorption

The effect of adsorbent dosage on Cr(VI) adsorption was investigated with adsorbent dosages of 0.01, 0.02, 0.05, 0.08, 0.1, and 0.2 g in 100 mL of chromate solution with a concentration of 2 mg·L^{-1} at 303 K. It can be seen in Fig. 3 that the adsorption efficiency (E) increased from 47.35% to 100% when the dosage of magnetic MWCNTs increased from 0.01 to 0.1 g. This finding agrees with the recent work by Kosa et al. (2012). When the adsorbent dosage increased, the equilibrium adsorption capacity (q_e) decreased considerably.
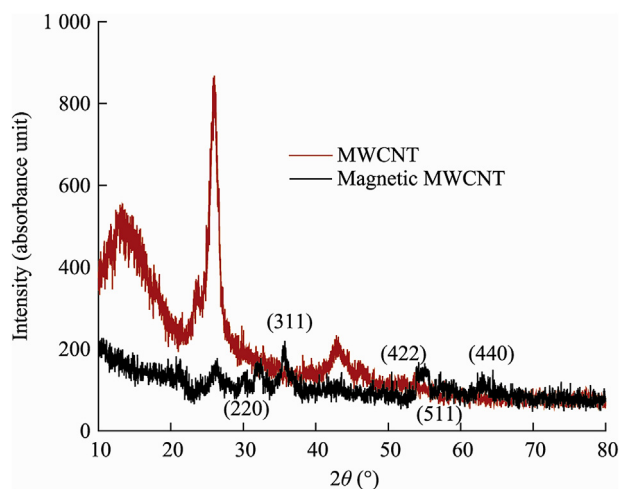
Consequently, 0.08 g of magnetic MWCNTs in 100 mL of solution with a concentration of 2 mg·L^{-1} was considered optimal for the Cr(VI) adsorption.

3.3. Effect of initial chromate concentration on Cr(VI) adsorption

The effect of the initial chromate concentration on Cr(VI) adsorption by the magnetic MWCNTs is shown in Fig. 4.

It can be seen that the equilibrium adsorption capacity increased almost linearly when the concentration of chromate solution increased from 0.78 to 25 mg·L^{-1}. This phenomenon can be explained in terms of the interaction between Cr(VI) ions and the adsorbent. There is a determinate amount of active adsorption sites on the surface of the adsorbent when adsorbent dosage is constant. When the amount of Cr(VI) per unit volume of solution increases, the ratio of the amount of Cr(VI) ions to the available adsorption sites also increases and more Cr(VI) ions in solution can be adsorbed by magnetic MWCNTs, giving rise to the increase of the equilibrium adsorption capacity. Similar phenomena have been observed in the adsorption of cadmium by activated palygorskite (Wang et al., 2007).
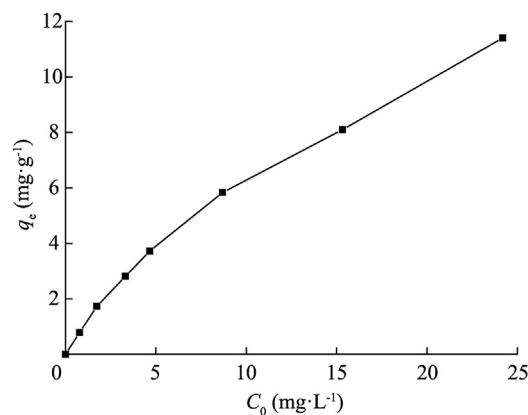

Fig. 2. XRD patterns of MWCNT and magnetic MWCNT.

Fig. 4. Effect of initial chromate concentration on Cr(VI) adsorption.

3.4. Adsorption kinetics

Fig. 5 shows the effect of contact time on Cr(VI) adsorption by the magnetic MWCNTs. It can be noted that Cr(VI) adsorption increased with contact time and initial chromate concentration. In order to describe adsorption kinetics, three commonly used kinetic models, the pseudo first-order kinetic model (Lagergren, 1898), pseudo second-order kinetic model (Ho and Mckay, 1999), and intraparticle diffusion model (Weber and Morris, 1963), were used to test the experimental data.

The pseudo first-order kinetic model and pseudo second-order kinetic model may be represented by Eq. (3) and Eq. (4), respectively:

$$\ln(q_e - q_t) = \ln q_e - k_1 t \tag{3}$$

$$\frac{t}{q_t} = \frac{1}{k_2 q_e^2} + \frac{t}{q_e} \tag{4}$$

where q_t is the amount of Cr(VI) adsorbed at time t (min), k_1 is the rate constant of the pseudo first-order adsorption process (min^{-1}), and k_2 is the rate constant of the pseudo second-order adsorption process (g·mg^{-1}·min^{-1}). The rate constants and correlation coefficients (r) are shown in Table 1.

The results show that the values calculated using the pseudo second-order model are closer to measured values than those using the pseudo first-order model. The values of the correlation coefficients indicate that the adsorption reaction is not a pseudo first-order process but a pseudo second-order process. This kind of phenomenon is common (Fasfous et al., 2010; Yao et al., 2012). The equilibrium adsorption capacity must be identified before calculation of the parameters of the pseudo first-order model, but this is difficult in practice. The pseudo second-order model contains all the adsorption processes: external liquid film diffusion, surface adsorption, and intraparticle diffusion; it can reflect the adsorption mechanism of Cr(VI) by the magnetic MWCNTs.
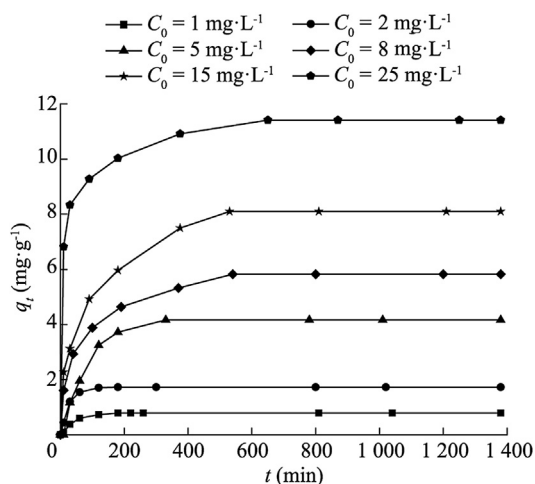

Fig. 5. Effect of contact time on chromate adsorption by magnetic MWCNTs at different initial chromate concentrations.

The intraparticle diffusion model can be described in Eq. (5):

$$q_t = k_p t^{0.5} + C \tag{5}$$

where k_p is the intraparticle diffusion rate constant (mg·g^{-1}·min$^{-0.5}$), and the intercept C is determined by extrapolation of the linear section of the curve of q_t versus $t^{0.5}$ (Fig. 6).

The plots of q_t versus $t^{0.5}$ in Fig. 6 can be divided into multiple linearity parts, which indicates that two or more processes occur during the adsorption process (Chen et al., 2007, 2009). In the first part, from 0 to 60 min, Cr(VI) is transported to the external surface of the adsorbent through a film diffusion process. The second linearity part shows a gradual adsorption process, which corresponds to the Cr(VI) ions diffusing into the adsorbent's surface pore. The third part is the final equilibrium stage, in which the intraparticle diffusion starts to slow down due to the extremely low concentration of the solution (Sun and Yang, 2003). Due to all the above, film diffusion and intraparticle diffusion simultaneously affect the adsorption of Cr(VI) ions by the magnetic MWCNTs.

3.5. Adsorption isotherms

The adsorption isotherms at 293 K, 303 K, 323 K, and 343 K are shown in Fig. 7. The equilibrium adsorption capacity increased with the temperature, indicating that the adsorption is an endothermic process. Two traditional adsorption isotherm models, the Langmuir model (Zhang and Wang, 2010) and the Freundlich model (Jeppu and Clement, 2012; Mittal et al., 2010a), were used to describe the adsorption process of Cr(VI) by the magnetic MWCNTs.

The Langmuir isotherm model can be expressed in Eq. (6):

$$\frac{C_e}{q_e} = \frac{1}{q_m K_L} + \frac{C_e}{q_m} \tag{6}$$

where q_m is the maximum amounts adsorbed (mg·g^{-1}), and K_L is the Langmuir adsorption constant (L·mg^{-1}) related to the free energy of adsorption.

The Freundlich isotherm model is an empirical equation. The linear equation of the Freundlich isotherm model is described in Eq. (7):

$$\ln q_e = \ln K_F + \frac{1}{n}\ln C_e \tag{7}$$

where K_F is the Freundlich adsorption constant (mg·g^{-1}) related to bond strength, and n is the nonlinearity parameter. K_F and $1/n$ can be determined from the intercept and slope of the straight line.

Table 2 shows both the Freundlich and Langmuir isotherm model parameters for the adsorption of Cr(VI). As can be seen from the correlation coefficients, the process can be better modeled with the Langmuir model. The maximum adsorbed amounts (q_m) increased from 12.531 to 16.234 mg·g^{-1} when

Table 1
Kinetic parameters for chromate adsorption by magnetic MWCNTs.

C_0 (mg·L^{-1})	Experiment	Pseudo first-order model			Pseudo second-order model		
	q_e (mg·g^{-1})	q_e (mg·g^{-1})	k_1 (min^{-1})	r	q_e (mg·g^{-1})	k_2 (g·mg^{-1}·min^{-1})	r
1	0.789	0.792	0.021 6	0.993 3	0.799	0.097 30	0.999 6
2	1.729	1.680	0.035 5	0.997 6	1.747	0.055 90	0.999 7
5	4.165	4.477	0.012 9	0.996 4	4.320	0.005 99	0.998 6
8	5.828	4.332	0.006 2	0.955 9	6.042	0.003 96	0.999 3
15	8.099	6.543	0.006 4	0.982 3	8.438	0.002 48	0.998 9
25	11.413	5.428	0.006 8	0.851 6	11.571	0.005 27	0.999 8

the temperature increased from 293 K to 343 K. A possible explanation is that high temperature extends the pore volume and surface area and provides more chances for Cr(VI) ions to pass the external boundary layer and penetrate more easily.

3.6. Adsorption thermodynamics

The thermodynamics parameters, such as the Gibbs free energy (ΔG), enthalpy (ΔH), and entropy (ΔS) for the adsorption process were obtained using the following formulas:

$$\ln \frac{q_e}{C_e} = -\frac{\Delta H}{RT} + \frac{\Delta S}{R} \tag{8}$$

$$\Delta G = \Delta H - T\Delta S \tag{9}$$

where R is defined as the ideal gas constant (kJ·mol^{-1}·K^{-1}), and T is temperature (K). The enthalpy and entropy were calculated from the slope and intercept of the plot of $\ln(q_e/C_e)$ versus $1/T$ (Table 3).

In Table 3, the positive value of ΔH shows the endothermic nature of the process. The negative values of ΔG show that the Cr(VI) adsorption is spontaneous. In general, the values of ΔG between 0 and -20 kJ·mol^{-1} indicate physical adsorption (Kuo et al., 2008), and the chemical adsorption occurs when the ΔG value is in the range of -80 to -400 kJ·mol^{-1}. The experimental data was derived to show that the adsorption process of Cr(VI) by magnetic MWCNTs was mainly physical adsorption.

3.7. Effect of pH value on Cr(VI) adsorption

The pH value is one of the most important parameters controlling the Cr(VI) adsorption process. In order to determine the adsorption behavior of Cr(VI), tests were conducted under constant experimental conditions, with an initial chromate concentration of 25 mg·L^{-1}. The effects of the pH value on the adsorption of Cr(VI) were examined when the pH value was in the range of 3.0−9.0, and the results are shown in Fig. 8.
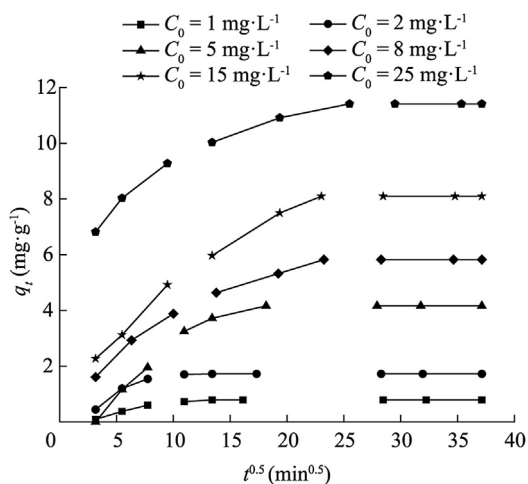

Fig. 6. Intraparticle diffusion kinetic plot for adsorption of Cr(VI) by magnetic MWCNTs.
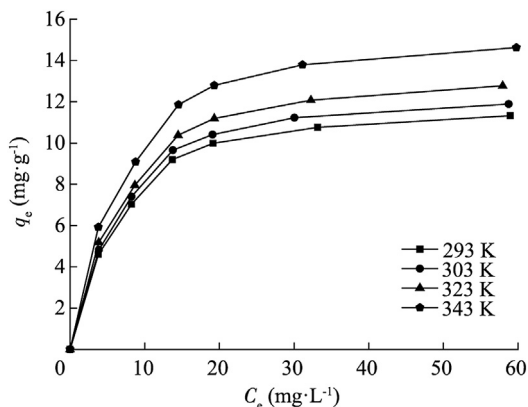

Fig. 7. Adsorption isotherm of Cr(VI) by magnetic MWCNTs.

Table 2
Freundlich and Langmuir isotherm model parameters.

Temperature (K)	Langmuir model			Freundlich model		
	q_m (mg·g^{-1})	K_L (L·mg^{-1})	r	K_F (mg·g^{-1})	n	r
293	12.531	0.174 0	0.998 6	3.413	3.053	0.883 5
303	13.158	0.173 2	0.998 5	3.547	3.010	0.880 9
323	14.205	0.165 4	0.998 7	3.750	2.986	0.895 6
343	16.234	0.166 5	0.998 7	4.308	3.002	0.894 9

Table 3
Thermodynamic parameters for Cr(VI) adsorption by magnetic MWCNTs.

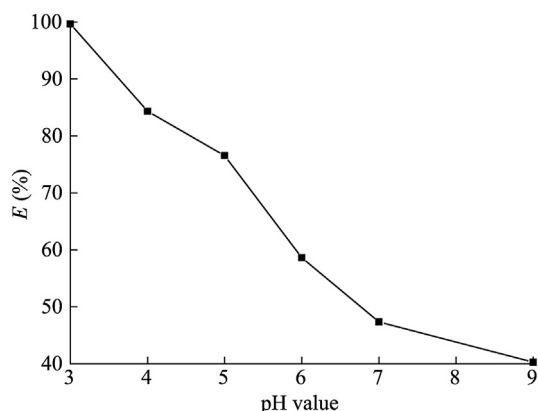| Temperature (K)	ΔH (kJ·mol^{-1})	ΔG (kJ·mol^{-1})	ΔS (J·mol^{-1}·K^{-1})
293	3.835	−0.803	15.828
303		−0.961	
323		−1.277	
343		−1.594	

Fig. 8. Effects of pH value of solution on Cr(VI) adsorption by magnetic MWCNTs.

The results indicate that the removal of Cr(VI) by magnetic MWCNTs was highly dependent on the pH value of the solution. The adsorption capacity was found to decrease with increasing pH values from 3.0 to 9.0. This phenomenon can be explained by the presence of different forms of Cr(VI) in the aqueous phase. The dominant forms of Cr(VI) were $Cr_2O_7^{2-}$ and $HCrO_4^-$ ions in the pH range of 3.0−7.0. At low pH values, the surface of magnetic MWCNTs became positively charged due to protonation, and the electrostatic forces between the magnetic MWCNTs and the negatively charged $Cr_2O_7^{2-}$ and $HCrO_4^-$ ions enhanced Cr(VI) adsorption (Li and Bowman, 2001). At higher pH values, CrO_4^{2-} ions prevailed in the solution. The affinity of CrO_4^{2-} ions for the magnetic MWCNTs was probably lesser than that of $Cr_2O_7^{2-}$ and $HCrO_4^-$ ions. As an additional effect, the protonation decreased with the increase of the pH value. Therefore, the adsorption efficiency decreased.

4. Conclusions

The magnetic MWCNTs exhibited excellent adsorption of Cr(VI). From the results of Cr(VI) adsorption by magnetic MWCNTs at different experimental conditions, the following conclusions can be drawn:

(1) In a batch of adsorption studies, the efficiency of Cr(VI) adsorption by magnetic MWCNTs increased with adsorbent dosage, but the equilibrium adsorption capacity decreased significantly.

(2) The equilibrium adsorption capacity increased almost linearly with the concentration of chromate solution.

(3) An adsorption kinetic experiment revealed that the adsorption of Cr(VI) by magnetic MWCNTs can be well described by the pseudo second-order kinetic model.

(4) The adsorption isotherms indicated that the Langmuir model better reflected the adsorption process than the Freundlich model.

(5) The thermodynamic function calculation revealed that the adsorption was a spontaneous process. Because of the positive value of enthalpy, Cr(VI) adsorption is an endothermic process. The Gibbs free energy of the adsorption decreased with the increase of the temperature.

(6) The adsorption mechanisms were associated with the forms of Cr(VI) in the aqueous phase. The adsorption capacity was found to decrease with increasing pH value.

References

Ahalya, N., Ramachandra, T.V., Kanamadi, R.D., 2003. Biosorption of heavy metals. Res. J. Chem. Environ. 7(4), 71−78.

Altas, L., Büyükgüngör, H., 2008. Sulfide removal in petroleum refinery wastewater by chemical precipitation. J. Hazard. Mater. 153(1−2), 462−469. http://dx.doi.org/10.1016/j.jhazmat.2007.08.076.

Benhammou, A., Yaacoubi, A., Nibou, L., Tanouti, B., 2007. Chromium(VI) adsorption from aqueous solution onto Moroccan Al-pillared and cationic surfactant stevensite. J. Hazard. Mater. 140(1−2), 104−109. http://dx.doi.org/10.1016/j.jhazmat.2006.06.077.

Chen, G.C., Shan, X.Q., Zhou, Y.Q., Shen, X.E., Huang, H.L., Khan, S.U., 2009. Adsorption kinetics, isotherms and thermodynamics of atrazine on surface oxidized multiwalled carbon nanotubes. J. Hazard. Mater. 169(1−3), 912−918. http://dx.doi.org/10.1016/j.jhazmat.2009.04.034.

Chen, H., Zhao, Y.G., Wang, A.Q., 2007. Removal of Cu(II) from aqueous solution by adsorption onto acid-activated palygorskite. J. Hazard. Mater. 149(2), 346−354. http://dx.doi.org/10.1016/j.jhazmat.2007.03.085.

Di, Z.C., Li, Y.H., Luan, Z.K., Liang, J., 2004. Adsorption of chromium(VI) ions from water by carbon nanotubes. Adsorpt. Sci. Technol. 22(6), 467−474. http://dx.doi.org/10.1260/0263617042879537.

Fasfous, I.I., Radwan, E.S., Dawoud, J.N., 2010. Kinetics, equilibrium and thermodynamics of the sorption of tetrabromobisphenol A on multiwalled carbon nanotubes. Appl. Surf. Sci. 256(23), 7246−7252. http://dx.doi.org/10.1016/j.apsusc.2010.05.059.

Gong, J.L., Wang, B., Zeng, G.M., Yang, C.P., Niu, C.G., Niu, Q.Y., Zhou, W.J., Liang, Y., 2009. Removal of cationic dyes from aqueous solution using magnetic multi-wall carbon nanotube nanocomposite as adsorbent. J. Hazard. Mater. 164(2−3), 1517−1522. http://dx.doi.org/10.1016/j.jhazmat.2008.09.072.

Gupta, V.K., Mittal, A., Kurup, L., Mittal, J., 2006. Adsorption of a hazardous dye, erythrosine, over hen feathers. J. Colloid Interface Sci. 304(1), 52−57. http://dx.doi.org/10.1016/j.jcis.2006.08.032.

Gupta, V.K., Jain, R., Mittal, A., Mathur, M., Sikarwar, S., 2007a. Photochemical degradation of the hazardous dye Safranin-T using TiO₂ catalyst. J. Colloid Interface Sci. 309(2), 464−469. http://dx.doi.org/10.1016/j.jcis.2006.12.010.

Gupta, V.K., Jain, R., Varshney, S., 2007b. Electrochemical removal of the hazardous dye Reactofix Red 3 BFN from industrial effluents. J. Colloid Interface Sci. 312(2), 292−296. http://dx.doi.org/10.1016/j.jcis.2007.03.054.

Gupta, V.K., Agarwal, S., Saleh, T.A., 2011a. Synthesis and characterization of alumina-coated carbon nanotubes and their application for lead removal. J. Hazard. Mater. 185(1), 17−23. http://dx.doi.org/10.1016/j.jhazmat.2010.08.053.

Gupta, V.K., Agarwal, S., Saleh, T.A., 2011b. Chromium removal by combining the magnetic properties of iron oxide with adsorption properties of carbon nanotubes. Water Res. 45(6), 2207−2212. http://dx.doi.org/10.1016/j.watres.2011.01.012.

Ho, Y.S., McKay, G., 1999. Pseudo-second order model for sorption processes. Process Biochem. 34(5), 451−465. http://dx.doi.org/10.1016/S0032-9592(98)00112-5.

Jeppu, G.P., Clement, T.P., 2012. A modified Langmuir-Freundlich isotherm model for simulating pH-dependent adsorption effects. J. Contam. Hydrol. 129−130, 46−53. http://dx.doi.org/10.1016/j.Jconhyd.2011.12.001.

Juang, R.S., Shiau, R.C., 2000. Metal removal from aqueous solutions using chitosan-enhanced membrane filtration. J. Membr. Sci. 165(2), 159−167. http://dx.doi.org/10.1016/S0376-7388(99)00235-5.

Kosa, S.A., Al-Zhrani, G., Salam, M.A., 2012. Removal of heavy metals from aqueous solutions by multi-walled carbon nanotubes modified with 8-

hydroxyquinoline. Chem. Eng. J. 181−182, 159−168. http://dx.doi.org/10.1016/j.cej.2011.11.044.

Kuo, C.Y., Wu, C.H., Wu, J.Y., 2008. Adsorption of direct dyes from aqueous solutions by carbon nanotubes: Determination of equilibrium, kinetics and thermodynamics parameters. J. Colloid Interface Sci. 327(2), 308−315. http://dx.doi.org/10.1016/j.jcis.2008.08.038.

Lagergren, S., 1898. About the theory of so-called adsorption of soluble substances, Kungliga Svenska Vetenskapsakademiens. Handlingar 24, 1−39.

Li, Y.H., Wang, S.G., Zhang, X.F., Wei, J.Q., Xu, C.L., Luan, Z.K., Wu, D.H., 2003. Adsorption of fluoride from water by aligned carbon nanotubes. Mater. Res. Bull. 38(3), 469−476. http://dx.doi.org/10.1016/S0025-5408(02)01063-2.

Li, Z.H., Bowman, R.S., 2001. Retention of inorganic oxyanions by organo-kaolinite. Water Res. 35(16), 3771−3776. http://dx.doi.org/10.1016/S0043-1354(01)00120−8.

Lu, C., Chiu, H., 2006. Adsorption of zinc(II) from water with purified carbon nanotubes. Chem. Eng. Sci. 61(4), 1138−1145. http://dx.doi.org/10.1016/j.ces.2005.08.007.

Madrakian, T., Afkhami, A., Ahmadi, M., 2011. Removal of some cationic dyes from aqueous solutions using magnetic-modified multi-walled carbon nanotubes. J. Hazard. Mater. 196, 109−114. http://dx.doi.org/10.1016/j.jhazmat.2011.08.078.

Mauter, M.S., Elimelech, M., 2008. Environmental applications of carbon-based nanomaterials. Environ. Sci. Technol. 42(16), 5843−5859. http://dx.doi.org/10.1021/es8006904.

Mittal, A., Kurup, L., Gupta, V.K., 2005. Use of waste materials—Bottom Ash and De-Oiled Soya, as potential adsorbents for the removal of Amaranth from aqueous solutions. J. Hazard. Mater. 117(2−3), 171−178. http://dx.doi.org/10.1016/j.jhazmat.2004.09.016.

Mittal, A., Mittal, J., Malviya, A., 2010a. Adsorption of hazardous dye crystal violet from wastewater by waste materials. J. Colloid Interface Sci. 343(2), 463−473. http://dx.doi.org/10.1016/j.jcis.2009.11.060.

Mittal, A., Mittal, J., Malviya, A., Gupta, V.K., 2010b. Removal and recovery of chrysoidine Y from aqueous solutions by waste materials. J. Colloid Interface Sci. 344(2), 497−507. http://dx.doi.org/10.1016/j.jcis.2010.01.007.

Ngomsik, A.F., Bee, A., Draye, M., Cote, G., Cabuil, V., 2005. Magnetic nano- and microparticles for metal removal and environmental applications: A review. Comptes Rendus Chim. 8(6−7), 963−970. http://dx.doi.org/10.1016/j.crci.2005.01.001.

O'Brien, T.J., Ceryak, S., Patierno, S.R., 2003. Complexities of chromium carcinogenesis: Role of cellular response, repair and recovery mechanisms. Mutat. Res./Fundam. Mol. Mech. Mutagen. 533(1−2), 3−36. http://dx.doi.org/10.1016/j.mrfmmm.2003.09.006.

Qu, S., Huang, F., Yu, S., Chen, G., Kong, J.L., 2008. Magnetic removal of dyes from aqueous solution using multi-walled carbon nanotubes filled with Fe_2O_3 particles. J. Hazard. Mater. 160(2−3), 643−647. http://dx.doi.org/10.1016/j.jhazmat.2008.03.037.

Rahbari, M., Goharrizi, A.S., 2009. Adsorption of lead(II) from water by carbon nanotubes: Equilibrium, kinetics, and thermodynamics. Water Environ. Res. 81(6), 598−607.

Ren, X.M., Chen, C.L., Nagatsu, M., Wang, X.K., 2011. Carbon nanotubes as adsorbents in environmental pollution management: A review. Chem. Eng. J. 170(2−3), 395−410. http://dx.doi.org/10.1016/j.cej.2010.08.045.

Shaidan, N.H., Eldemerdash, U., Awad, S., 2012. Removal of Ni(II) ions from aqueous solutions using fixed-bed ion exchange column technique. J. Taiwan Inst. Chem. Eng. 43(1), 40−45. http://dx.doi.org/10.1016/j.jtice.2011.06.006.

Sun, Q., Yang, L.Z., 2003. The adsorption of basic dyes from aqueous solution on modified peat-resin particle. Water Res. 37(7), 1535−1544. http://dx.doi.org/10.1016/S0043-1354(02)00520-1.

Tang, W.W., Zeng, G.M., Gong, J.L., Liu, Y., Wang, X.Y., Liu, Y.Y., Liu, Z.F., Chen, L., Zhang, X.R., Tu, D.Z., 2012. Simultaneous adsorption of atrazine and Cu(II) from wastewater by magnetic multi-walled carbon nanotube. Chem. Eng. J. 211−212, 470−478. http://dx.doi.org/10.1016/j.cej.2012.09.102.

Tarigh, G.D., Shemirani, F., 2013. Magnetic multi-wall carbon nanotube nanocomposite as an adsorbent for preconcentration and determination of lead(II) and manganese(II) in various matrices. Talanta 115, 744−750. http://dx.doi.org/10.1016/j.talanta.2013.06.018.

Tawabini, B., Al-Khaldi, S., Atieh, M., Khaled, M.M., 2010. Removal of mercury from water by multi-walled carbon nanotubes. Water Sci. Technol. 61(3), 591−598. http://dx.doi.org/10.2166/wst.2010.897.

Wang, W.J., Chen, H., Wang, A.Q., 2007. Adsorption characteristics of Cd(II) from aqueous solution onto activated palygorskite. Sep. Purif. Technol. 55(2), 157−164. http://dx.doi.org/10.1016/j.seppur.2006.11.015.

Weber, W.J., Morris, J.C., 1963. Kinetics of adsorption on carbon from solution. J. Sanit. Eng. Div. 89(2), 31−60.

Yao, C., Xu, Y.Y., Kong, Y., Liu, W.J., Wang, W.J., Wang, Z.L., Wang, Y., Ji, J.L., 2012. Polypyrrole/palygorskite nanocomposite: A new chromate collector. Appl. Clay Sci. 67−68, 32−35. http://dx.doi.org/10.1016/j.clay.2012.07.007.

Yao, J., Tian, L., Wang, Y.X., Djah, A., Wang, F., Chen, H., Su, C., Zhuang, R., Zhou, Y., Choi, M.M., Bramanti, E., 2008. Microcalorimetric study the toxic effect of hexavalent chromium on microbial activity of Wuhan brown sandy soil: An in vitro approach. Ecotoxicol. Environ. Saf. 69(2), 289−295. http://dx.doi.org/10.1016/j.ecoenv.2007.02.005.

Zhang, P.K., Wang, L., 2010. Extended Langmuir equation for correlating multilayer adsorption equilibrium data. Sep. Purif. Technol. 70(3), 367−371. http://dx.doi.org/10.1016/j.seppur.2009.10.007.